

# Inverse-kinematics proton scattering on $^{50}\text{Ca}$ : determining effective charges using complementary probes

L. A. Riley,<sup>1</sup> M. L. Agiorgousis,<sup>1</sup> T.R. Baugher,<sup>2</sup> D. Bazin,<sup>2</sup> M. Bowry,<sup>2</sup> P. D. Cottle,<sup>3</sup> F. G. DeVone,<sup>1</sup> A. Gade,<sup>2</sup> M. T. Glowacki,<sup>1</sup> K. W. Kemper,<sup>3</sup> E. Lunderberg,<sup>2</sup> D. M. McPherson,<sup>3</sup> S. Noji,<sup>2</sup> F. Recchia,<sup>2,\*</sup> B. V. Sadler,<sup>1</sup> M. Scott,<sup>2</sup> D. Weisshaar,<sup>2</sup> and R. G. T. Zegers<sup>2,4</sup>

<sup>1</sup>*Department of Physics and Astronomy, Ursinus College, Collegeville, PA 19426, USA*

<sup>2</sup>*National Superconducting Cyclotron Laboratory, Michigan State University, East Lansing, MI, 48824, USA*

<sup>3</sup>*Department of Physics, Florida State University, Tallahassee, FL 32306, USA*

<sup>4</sup>*Joint Institute for Nuclear Astrophysics, Michigan State University, East Lansing, MI 48824, USA*  
(Dated: July 31, 2018)

We have performed measurements of the  $0_{\text{g.s.}}^+ \rightarrow 2_1^+$  excitations in the neutron-rich isotopes  $^{48,50}\text{Ca}$  via inelastic proton scattering on a liquid hydrogen target, using the GRETTINA  $\gamma$ -ray tracking array. A comparison of the present results with those from previous measurements of the lifetimes of the  $2_1^+$  states provides us the ratio of the neutron and proton matrix elements for the  $0_{\text{g.s.}}^+ \rightarrow 2_1^+$  transitions. These results allow the determination of the ratio of the proton and neutron effective charges to be used in shell model calculations of neutron-rich isotopes in the vicinity of  $^{48}\text{Ca}$ .

Isotopes within a few nucleons of the doubly-magic nuclei provide the foundation for the nuclear shell model. The simplicity of the wavefunctions of the valence nucleons in these nuclei allows the determination of the two-body matrix elements necessary for predicting the energies of excited states and the effective charges used in calculating transition strengths in a given shell-model space. Effective charges reflect the strength of the coupling between the motion of the valence nucleons and the virtual excitations of the core nucleons.

The neutron-rich exotic calcium isotopes beyond the doubly-magic nucleus  $^{48}\text{Ca}$  are particularly interesting because of shell effects caused by the filling of the  $p_{3/2}$  and  $p_{1/2}$  neutron orbits that are just above the major  $N = 28$  shell closure. As a result, the determination of the effective charges for these neutron-rich calcium isotopes is of particular interest. Valiente-Dobón *et al.* [1] addressed this by determining the electromagnetic strengths of the  $2_1^+ \rightarrow 0_{\text{g.s.}}^+$  transition in  $^{50}\text{Ca}$  and the transition between the ground state and 1065 keV  $11/2^-$  state in  $^{51}\text{Sc}$  via lifetime measurements. They examined two candidate sets of effective charges, one of which was recommended in an extensive shell model study of the  $fp$  shell [2] and another of which was extracted from an experimental study of the mirror nuclei  $^{51}\text{Fe}$  and  $^{51}\text{Mn}$  [3]. On the basis of their measurements, Valiente-Dobón *et al.* argued for the set from Ref. [2].

However, measurements of electromagnetic strengths only determine the proton transition matrix elements and do not determine the neutron transition matrix elements, which are particularly important in the case of  $^{50}\text{Ca}$ , because the only valence nucleons are neutrons when assuming an inert  $Z = 20$  proton core. Here we report the results of a measurement of the  $0_{\text{g.s.}}^+ \rightarrow 2_1^+$  excitation in  $^{50}\text{Ca}$  using the inelastic scattering of protons, for which the transition matrix element includes contributions from both protons and neutrons. The experiment

was performed in inverse kinematics with a beam of radioactive  $^{50}\text{Ca}$  ions. By comparing the results of the present proton-scattering measurement with the previous measurement of the electromagnetic matrix element deduced from the lifetime measurement of Ref. [1], we can determine the neutron transition matrix element and demonstrate that the proton effective charge must be approximately a factor of 3 larger than the neutron effective charge, which is consistent with the effective charges proposed by Honma *et al.* [2]. The determination of the neutron transition matrix element via the present proton scattering measurement significantly strengthens the assertion given in Ref. [1] that the effective charges proposed by Honma *et al.* are valid near  $^{48}\text{Ca}$ . We also report a similar measurement of  $^{48}\text{Ca}$  for which the proton-scattering deformation length has already been measured. [4–6]

The experiment was performed at the Coupled-Cyclotron Facility of the National Superconducting Cyclotron Laboratory at Michigan State University. A cocktail beam was produced by the fragmentation of a 130 MeV/u  $^{76}\text{Ge}$  primary beam in a 376 mg/cm<sup>2</sup>  $^9\text{Be}$  production target. The secondary products were separated by the A1900 fragment separator [7]. A 45 mg/cm<sup>2</sup> aluminum achromatic wedge was used to enhance separation of the cocktail by  $Z$ .

Secondary beam particles were identified upstream of the reaction target by energy loss in a silicon pin diode located at the object of the analysis line of the S800 magnetic spectrograph [8] and by time of flight from the A1900 extended focal plane to the S800 object scintillator. The beam then traversed the Ursinus College Liquid Hydrogen Target. The target, based on the design of Ryuto *et al.* [9], was installed at the pivot point of the S800. Beam-like reaction products were identified by energy loss in the S800 ion chamber and time of flight from the S800 object scintillator to a scintillator in the

focal plane of the S800. The secondary beam contained components spanning the range  $14 \leq Z \leq 23$ , including  $^{48,50}\text{Ca}$ , the subjects of the present work. A total of  $4.3 \times 10^8$  secondary beam particles traversed the reaction target in 114 hours. Of these,  $3.0 \times 10^7$  particles were tagged as  $^{50}\text{Ca}$  particles in both incoming and outgoing particle identification gates, and  $4.0 \times 10^6$  particles were tagged as  $^{48}\text{Ca}$ , corresponding to 73 particles per second and 9.3 particles per second, respectively.

The liquid hydrogen was contained in a 30 mm thick cylindrical aluminum target cell with 125  $\mu\text{m}$  Kapton entrance and exit windows. The cell was surrounded by a 1 mm thick aluminum radiation shield with entrance and exit windows covered by 5  $\mu\text{m}$  aluminized Mylar foil. The temperature and pressure of the target cell were maintained at 16.0 K and 868 Torr throughout the experiment. The Kapton windows were deformed by the pressure differential between the cell and the vacuum, adding to the nominal 30 mm target thickness.

The GRETINA [10]  $\gamma$ -ray tracking array, consisting of 28 36-fold segmented high purity germanium crystals packaged in seven clusters of four crystals each, was installed at the pivot point of the S800 in a configuration designed to accommodate the liquid hydrogen target. Two of the seven modules were mounted at  $58^\circ$ , four at  $90^\circ$ , and one at  $122^\circ$  with respect to the beam axis.

We used realistic GEANT4 [11] simulations to extract  $\gamma$ -ray yields from measured spectra. The simulation code includes detailed models of GRETINA and the liquid hydrogen target to account for scattering of  $\gamma$  rays by the dead material surrounding the liquid hydrogen and the active detector volumes. The code reproduces measured photopeak efficiencies within 5% between 300 keV and 3.5 MeV. In addition to  $\gamma$  rays, simulated beam particles are also tracked as they traverse the target and undergo  $\gamma$  decay in flight. The Kapton entrance and exit windows of the target cell bulged outward due to the 868 Torr pressure differential between the liquid hydrogen and the evacuated beamline. Therefore, the roughly 4 mm  $\times$  8 mm beam spot sampled a range of target thicknesses. We varied the thickness of the simulated window bulges to fit the kinetic energy distributions of the outgoing scattered beam particles measured with the S800 to determine an effective target thickness of 34.3 mm, corresponding to an areal density of 258 mg/cm<sup>2</sup>. The GEANT4 simulations described above were used to determine that inelastic scattering reactions took place at an average  $^{48}\text{Ca}$  beam energy of 98 MeV/u and an average  $^{50}\text{Ca}$  energy of 90 MeV/u. The corresponding beam velocities,  $v/c = 0.43$  and  $v/c = 0.41$ , were used in the Doppler reconstruction of the measured and simulated  $\gamma$ -ray spectra.

The Doppler-corrected  $\gamma$ -ray spectra collected in coincidence with inelastically scattered  $^{48}\text{Ca}$  and  $^{50}\text{Ca}$  beam particles are shown in Figure 1. The solid curve in each panel is a fit of a linear combination of GEANT4 sim-

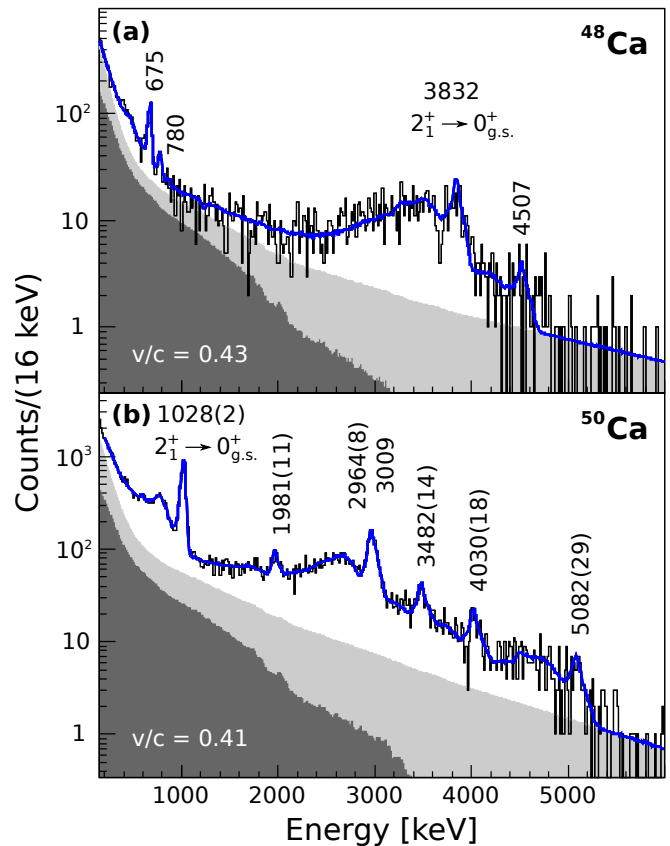


FIG. 1. (Color online) Doppler-corrected spectra of gamma rays measured in coincidence with incoming and outgoing (a)  $^{48}\text{Ca}$  and (b)  $^{50}\text{Ca}$  particles. The solid curves are the GEANT4 fits described in the text. The shaded region is the background, consisting of non-prompt (dark gray) and prompt (light gray) components.

ulations of the response of GRETINA to the observed  $\gamma$  rays and prompt and non-prompt background components, shaded in light gray and dark gray in the figure, respectively. The non-prompt background is due to random coincidences between scattered beam particles and the room background. We fit this component of the spectrum with a scaled room background measurement. The scaling is determined with a fit to the laboratory-frame spectrum and fixed in the projectile-frame fit. The remaining prompt component of the background, shaded in light gray in Figure 1, can be successfully accounted for by including two exponential functions in the projectile-frame fit. The  $\gamma$ -ray energies and intensities extracted from the fits are listed in Table I along with branching ratios.

In the case of  $^{48}\text{Ca}$ , we included in the fit all of the gamma rays de-exciting states up to an excitation energy of 6 MeV that are known [4–6] to be strongly-populated by proton scattering. We did not have sufficient statistics to independently determine the energies of the 648 keV, 1538 keV, and 4507 keV gamma rays,

and the 648/675 keV, 754/758 keV, and 863/867 keV doublets in the  $^{48}\text{Ca}$  spectrum were not well resolved in the measured spectrum. With the exception of the relatively intense 675 keV transition, we fixed the energies of these transitions at the adopted values [12] in the fit. Similarly, in the  $^{50}\text{Ca}$  spectrum, the 2964/3009 keV doublet is not resolved. We used the adopted energy [13] for the much fainter 3009 keV member of the doublet in the fit.

We observe a  $\gamma$ -ray at 5082(29) keV in  $^{50}\text{Ca}$  that has not been previously observed. We do not have sufficient statistics to place it in the level scheme on the basis of  $\gamma$ - $\gamma$  coincidence gating. The neutron separation energy in  $^{50}\text{Ca}$  is 6353(8) keV [13]. We therefore suspect that the 5082 keV  $\gamma$  ray feeds either the  $2_1^+$  state at 1027 keV or the ground state. Although its energy is compatible with a  $\gamma$  ray de-exciting the known state at 5110 keV, the tentative assignment of  $J^\pi = 5^-$  to this state suggests that it is unlikely to decay directly to the ground state.

A 22-hour empty-cell measurement was also made to study possible contamination of the  $\gamma$ -ray spectrum by reactions in the Kapton windows and aluminized Mylar foils. No discernible peaks were observed in the empty-cell spectra collected in coincidence with scattered  $^{48}\text{Ca}$  and  $^{50}\text{Ca}$  particles.

The uncertainties in both the position and velocity of the scattered beam particles undergoing  $\gamma$  decay in the thick target lead to significant Doppler broadening of the photopeaks in the Doppler-corrected spectrum. The photopeak of a  $\gamma$  ray de-exciting a state with a lifetime on the order of hundreds of picoseconds or more is further broadened due to the extended range of decay positions. The photopeak of the 1027 keV  $\gamma$  ray in the spectrum of  $^{50}\text{Ca}$  is slightly broadened relative to a simulated peak assuming zero lifetime for the  $2_1^+$  state. A best fit to the spectrum is obtained with a mean lifetime of  $\tau = 99(8)$  ps, in good agreement with the recoil distance Doppler shift method result from Ref. [1] of  $\tau = 96(3)$  ps for the  $2_1^+$  state of  $^{50}\text{Ca}$ .

Partial level schemes of  $^{48}\text{Ca}$  and  $^{50}\text{Ca}$  are shown in Figure 2. The established level schemes enable us to apply feeding corrections to the  $\gamma$ -ray cross sections to deduce the cross sections given in Table I for direct population of excited states via proton scattering. In the error range of the  $2_1^+$ -state cross section in  $^{50}\text{Ca}$ , we have accounted for the possibility that the unplaced 5082 keV  $\gamma$  ray feeds the  $2_1^+$  state.

We used the coupled-channels code ECIS95 [14] to extract proton-scattering deformation lengths from our measured cross sections for inelastic scattering to the  $2_1^+$  states of  $^{48,50}\text{Ca}$ . Using the global optical potential of Ref. [15] and treating the  $2_1^+$  states as quadrupole vibrations yields proton-scattering deformation lengths  $\delta_{2(p,p')} = 0.78(11)$  fm for  $^{48}\text{Ca}$  and  $0.57(9)$  fm for  $^{50}\text{Ca}$ . Using a rotational model for  $^{50}\text{Ca}$  yields  $\delta_{2(p,p')} = 0.56(9)$  fm. The discrepancy between the vibrational-

and rotational-model results is negligible compared with the experimental uncertainty.

The deformation length of the  $2_1^+$  state of  $^{48}\text{Ca}$  has been determined via distorted-wave Born approximation (DWBA) analyses of proton angular distributions over a broad range of proton energies —  $\delta_{2(p,p')} = 0.70(3)$  fm at 40 MeV [4],  $0.61(3)$  fm at 65 MeV [5], and  $0.61(2)$  fm at 500 MeV. [6]

The ratio of neutron to proton transition matrix elements,  $M_n$  and  $M_p$ , is related to the corresponding proton and neutron deformation lengths,  $\delta_n$  and  $\delta_p$ , by [16]

$$\frac{M_n}{M_p} = \frac{N\delta_n}{Z\delta_p}. \quad (1)$$

The lifetimes of the  $2_1^+$  states of  $^{48,50}\text{Ca}$  are known [1, 12] to be  $\tau = 38.7(19)$  fs and  $96(3)$  ps. These purely electromagnetic measurements give the proton deformation lengths  $\delta_p = 0.479(13)$  fm and  $0.304(4)$  fm directly. Proton scattering is sensitive to protons as well as to neutrons. Hence the proton-scattering deformation lengths from the present work can be combined with the proton deformation lengths to determine  $M_n/M_p$  for the  $2_1^+$  states. The deformation length measured using a probe  $F$  with a mixed sensitivity to protons and neutrons is related to the neutron and proton deformation lengths via [17]

$$\delta_F = \frac{b_n^F N \delta_n + b_p^F Z \delta_p}{b_n^F N + b_p^F Z}, \quad (2)$$

where  $b_n^F$  ( $b_p^F$ ) are the external-field neutron (proton) interaction strengths of the probe. In the case of a pure electromagnetic probe combined with proton scattering, Eqs. (1) and (2) yield

$$\frac{M_n}{M_p} = \frac{b_p}{b_n} \left( \frac{\delta_{(p,p')}}{\delta_p} \left( 1 + \frac{b_n N}{b_p Z} \right) - 1 \right). \quad (3)$$

The ratio  $b_n/b_p$  is approximately 3 for proton scattering below 50 MeV and approximately 1 at 1 GeV [17], but it is not well-determined at the intermediate beam energies of the present work.

Values of  $M_n/M_p$  for the  $2_1^+$  state of  $^{48}\text{Ca}$ , calculated using  $b_n/b_p = 1$  and  $b_n/b_p = 3$ , are  $2.5(4)$  and  $2.9(6)$ , respectively. These results span the range  $2.1 \leq M_n/M_p \leq 3.5$ . Lacking a firm value of  $b_n/b_p$ , we adopt the result  $M_n/M_p = 2.8(7)$  to cover this range. For  $^{50}\text{Ca}$ , an identical analysis gives  $M_n/M_p = 3.5(9)$ . These results along with the  $M_n/M_p$  values of  $2_1^+$  states in the neutron-rich calcium isotopes from Ref. [16] are shown in Figure 3.

In a nucleus like  $^{50}\text{Ca}$  that has only valence neutrons, the ratio  $M_n/M_p$  can be shown in a straightforward way to be equal to the ratio of the shell model effective charges  $e_p/e_n$  under a reasonable assumption — that the coupling between valence neutrons and core neutrons has the same strength as the coupling between valence and core

TABLE I. Level energies, spins and parities, and  $\gamma$ -ray energies from Refs. [12, 13],  $\gamma$ -ray energies, intensities relative to that of the  $2_1^+ \rightarrow 0_{g.s.}^+$  transitions, branching ratios (BR), and cross sections from the present work.

	Refs. [12, 13]				Present work			
	$E_{\text{level}}$ [keV]	$J^\pi$ [ $\hbar$ ]	$E_\gamma$ [keV]	BR [%]	$E_\gamma$ [keV]	$I_\gamma$ [%]	BR [%]	$\sigma$ [mb]
$^{48}\text{Ca}$	3831.72(6)	$2^+$	3832.2(5)		3842(12)	100(5)		5.2(19)
	4506.78(5)	$3^-$	675.05(7)	80.0(14)	678(2)	45(6)	72(7)	6.8(14)
			4507.3(5)	20.0(16)	4507	17(3)	28(7)	
	4611.81(7)	$3(+)$	780.25(15)		782(8)	12(3)		< 3.2
	5260.41(8)	$4(-)$	648.4(1)	86(5)	648	12(4)	69(15)	< 1.9
			753.8(1)	14(5)	754	5(3)	31(15)	
	5369.59(6)	$3-$	757.5(1)		758	–		< 1.1
			862.7(1)		863	4.7(30)		
		866.9(1)		867	< 3			
		1537.8(1)		1538	2.4(30)			
$^{50}\text{Ca}$	1026.7(1)	$2^+$	1026.7(1)		1028(2)	100(5)		3.4(11)
	3002.1(5)	$(2^+)$	1975.3(5)		1981(11)	9(1)		1.4(2)
	3997.1(2)	$(3^-)$	2970.2(2)		2964(8)	42(4)		6.8(6)
	4035.7(4)	$(1^+, 2^+)$	4035.6(5)	62(1)	4030(18)	12(3)	44(12)	3.5(7)
			3008.9(5)	38(2)	3009	9(3)	56(15)	
	4515.0(1)	$(4^+)$	3488.2(1)		3482(14)	13(1)		1.6(2)
	5109.8(2)	$(5^-)$	594.8(1)		603(11)	2.6(9)		0.4(1)
					5082(29)	5.4(6)		

(a)

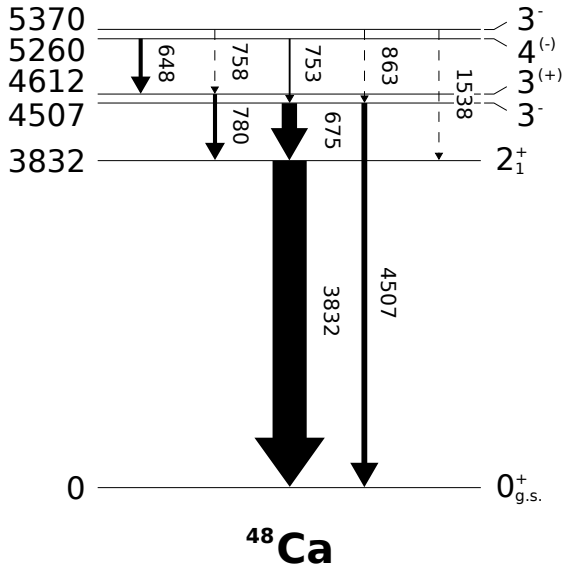
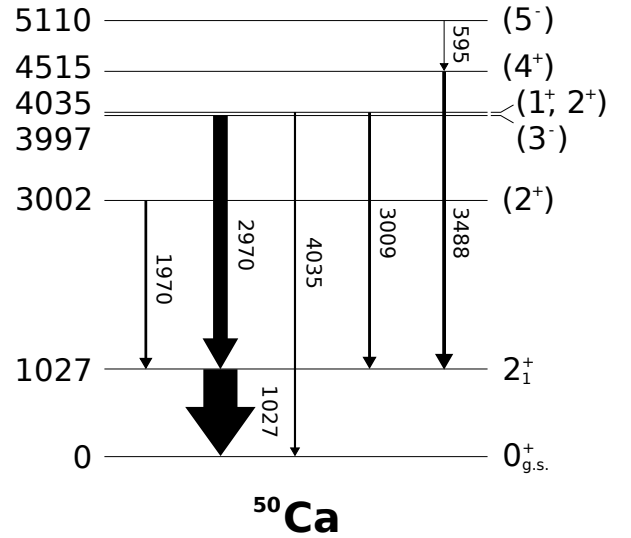
(b) 6353 – – – – –  $S_n$ 

FIG. 2. Partial level schemes of (a)  $^{48}\text{Ca}$  from Ref. [12] and (b)  $^{50}\text{Ca}$  from Ref. [13], showing levels populated in the present work. Arrow widths are proportional to the measured  $\gamma$ -ray intensities.

protons. We start with the formalism given by Brown and Wildenthal [18] in which

$$M_p = A_p(1 + \delta_{pp}) + A_n\delta_{pn}, \quad (4)$$

$$M_n = A_n(1 + \delta_{nn}) + A_p\delta_{np}. \quad (5)$$

Here,  $A_p$  and  $A_n$  are the proton and neutron strength amplitudes, respectively, and the  $\delta_{ab}$  account for the cou-

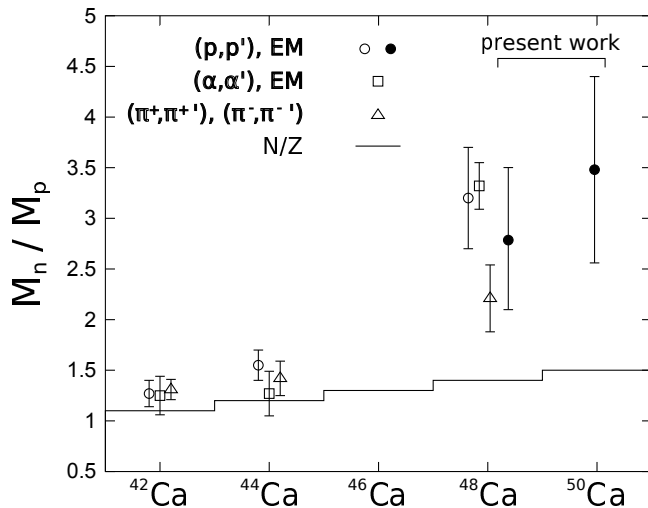


FIG. 3. The ratio of neutron to proton transition matrix elements  $M_n/M_p$  in the neutron-rich calcium isotopes. The open symbols are taken from Ref. [16] and the filled circles are from the present work.

pling of the nucleons  $b$  of the model space to the virtual excitations of the core nucleons  $a$ . In  $^{50}\text{Ca}$ , there are no valence protons so that  $A_p = 0$  and

$$\frac{M_n}{M_p} = \frac{1 + \delta_{nn}}{\delta_{pn}}. \quad (6)$$

If we assume that  $\delta_{nn} = \delta_{pp}$  then the conventional model space proton effective charge  $e_p$  is given by

$$e_p = 1 + \delta_{pp} = 1 + \delta_{nn}. \quad (7)$$

With the conventional definition of the neutron effective charge  $e_n = \delta_{pn}$ , we have

$$\frac{e_p}{e_n} = \frac{M_n}{M_p}. \quad (8)$$

Honma *et al.* [2] adopted  $e_p = 1.5$  and  $e_n = 0.5$ , which gives  $e_p/e_n = 3.0$ . In contrast, du Rietz *et al.* [3] concluded from their study of  $^{51}\text{Fe}$  and  $^{51}\text{Mn}$  that  $e_p = 1.15$  and  $e_n = 0.80$ , giving  $e_p/e_n = 1.4$ . The present result,  $e_p/e_n = 3.5(9)$ , clearly favors the effective charges selected by Honma *et al.*, in agreement with Valiente-Dobón *et al.* [1]. This does not mean that the conclusion of du Rietz *et al.* regarding effective charges is incorrect. Instead, it indicates that the effective charges in the neutron-rich isotopes in the vicinity of  $^{48}\text{Ca}$  are different than they are near the  $N \approx Z$  nuclei,  $^{51}\text{Fe}$  and  $^{51}\text{Mn}$ . Indeed, an isospin dependence in effective charges was argued a long time ago by Bohr and Mottelson in Ref. [19].

In summary, we have performed a measurement of inelastic proton scattering in inverse kinematics on the neutron-rich isotopes  $^{48,50}\text{Ca}$ . Through a comparison

of the proton-scattering deformation lengths from the present work with previous lifetime measurements, we determined the ratio of the neutron and proton matrix elements for the  $0_{g.s.}^+ \rightarrow 2_1^+$  transitions in these nuclei. The  $M_n/M_p$  value for  $^{48}\text{Ca}$  is in good agreement with prior results. Our result for  $^{50}\text{Ca}$  allows us for the first time to determine the ratio of the proton and neutron effective charges in the  $fp$  shell for isotopes in the vicinity of  $^{48}\text{Ca}$  and to conclude that the effective charges adopted for these nuclei by Honma *et al.* [2] are appropriate for use in shell model calculations in this region.

We are grateful for conversations with B.A. Brown. We also thank T.J. Carroll for the use of the Ursinus College Parallel Computing Cluster, which is supported by NSF grant no. PHY-1205895. This work was supported by the National Science Foundation under Grant Nos. PHY-1303480, PHY-1064819, and PHY-1102511. GRETINA was funded by the US DOE - Office of Science. Operation of the array at NSCL is supported by NSF under Cooperative Agreement PHY-1102511(NSCL) and DOE under grant DE-AC02-05CH11231(LBNL).

\* Dipartimento di Fisica e Astronomia Galileo Galilei, Università degli Studi di Padova, I-35131 Padova, Italy

- [1] J. J. Valiente-Dobón, D. Mengoni, A. Gadea, E. Farnea, S. M. Lenzi, S. Lunardi, A. Dewald, Th. Pissulla, S. Szilner, R. Broda, F. Recchia, A. Algora, L. Angus, D. Bazzacco, G. Benzoni, P. G. Bizzeti, A. M. Bizzeti-Sona, P. Boutachkov, L. Corradi, F. Crespi, G. de Angelis, E. Fioretto, A. Görgen, M. Gorska, A. Gottardo, E. Grodner, B. Guiot, A. Howard, W. Krolas, S. Leoni, P. Mason, R. Menegazzo, D. Montanari, G. Montagnoli, D. R. Napoli, A. Obertelli, T. Pawlat, G. Pollarolo, B. Rubio, E. Sahin, F. Scarlassara, R. Silvestri, A. M. Stefanini, J. F. Smith, D. Steppenbeck, C. A. Ur, P. T. Wady, J. Wrzesinski, E. Maglione, and I. Hamamoto, Phys. Rev. Lett. **102**, 242502 (2009).
- [2] M. Honma, T. Otsuka, B. A. Brown, and T. Mizusaki, Phys. Rev. C **69**, 034335 (2004).
- [3] R. du Rietz, J. Ekman, D. Rudolph, C. Fahlander, A. Dewald, O. Möller, B. Saha, M. Axiotis, M. A. Bentley, C. Chandler, G. de Angelis, F. Della Vedova, A. Gadea, G. Hammond, S. M. Lenzi, N. Märginean, D. R. Napoli, M. Nespolo, C. Rusu, and D. Tonev, Phys. Rev. Lett. **93**, 222501 (2004).
- [4] C. R. Gruhn, T. Y. T. Kuo, C. J. Maggiore, and B. M. Preedom, Phys. Rev. C **6**, 944 (1972).
- [5] Y. Fujita, M. Fujiwara, S. Morinobu, T. Yamazaki, T. Itahashi, H. Ikegami, and S. I. Hayakawa, Phys. Rev. C **37**, 45 (1988).
- [6] K. K. Seth, D. Barlow, A. Saha, R. Soundranayagam, S. Iversen, M. Kaletka, M. Basko, D. Smith, G. W. Hoffmann, M. L. Barlett, R. Fergerson, J. McGill, and E. C. Milner, Physics Letters B **158**, 23 (1985).
- [7] D. J. Morrissey, B. M. Sherrill, M. Steiner, A. Stolz, and I. Wiedenhöver, Nucl. Instrum. Methods Phys. Res. B **204**, 90 (2003).

- [8] D. Bazin, J. A. Caggiano, B. M. Sherrill, J. Yurkon, and A. Zeller, *Nucl. Instrum. Methods Phys. Res. B* **204**, 629 (2003).
- [9] H. Ryuto, M. Kunibu, T. Minemura, T. Motobayashi, K. Sagara, S. Shimoura, M. Tamaki, Y. Yanagisawa, and Y. Yano, *Nucl. Instrum. Methods Phys. Res. A* **555**, 1 (2005).
- [10] S. Paschalis, I. Y. Lee, A. O. Macchiavelli, C. M. Campbell, M. Cromaz, S. Gros, J. Pavan, J. Qian, R. M. Clark, H. L. Crawford, D. Doering, P. Fallon, C. Lionberger, T. Loew, M. Petri, T. Stezelberger, S. Zimmermann, D. C. Radford, K. Lagergren, D. Weisshaar, R. Winkler, T. Glasmacher, J. T. Anderson, and C. W. Beausang, *Nucl. Instrum. Methods Phys. Res. A* **709**, 44 (2013).
- [11] S. Agostinelli, J. Allison, K. Amako, J. Apostolakis, H. Araujo, P. Arce, M. Asai, D. Axen, S. Banerjee, G. Barrand, F. Behner, L. Bellagamba, J. Boudreau, L. Broglia, A. Brunengo, H. Burkhardt, S. Chauvie, J. Chuma, R. Chytrcek, G. Cooperman, G. Cosmo, P. Degtyarenko, A. Dell'Acqua, G. Depaola, D. Dietrich, R. Enami, A. Feliciello, C. Ferguson, H. Fesefeldt, G. Folger, F. Foppiano, A. Forti, S. Garelli, S. Giani, R. Giannitrapani, D. Gibin, J. J. G. Cadenas, I. González, G. G. Abril, G. Greeniaus, W. Greiner, V. Grichine, A. Grossheim, S. Guatelli, P. Gumplinger, R. Hamatsu, K. Hashimoto, H. Hasui, A. Heikkinen, A. Howard, V. Ivanchenko, A. Johnson, F. W. Jones, J. Kallenbach, N. Kanaya, M. Kawabata, Y. Kawabata, M. Kawaguti, S. Kelner, P. Kent, A. Kimura, T. Kodama, R. Kokoulin, M. Kossov, H. Kurashige, E. Lamanna, T. Lampen, V. Lara, V. Lefebvre, F. Lei, M. Liendl, W. Lockman, F. Longo, S. Magni, M. Maire, E. Medernach, K. Minamimoto, P. M. de Freitas, Y. Morita, K. Murakami, M. Nagamatu, R. Nartallo, P. Nieminen, T. Nishimura, K. Ohtsubo, M. Okamura, S. O'Neale, Y. Oohata, K. Paeck, J. Perl, A. Pfeiffer, M. G. Pia, F. Ranjard, A. Rybin, S. Sadilov, E. D. Salvo, G. Santin, T. Sasaki, N. Savvas, Y. Sawada, S. Scherer, S. Sei, V. Sirotenko, D. Smith, N. Starkov, H. Stoecker, J. Sulkimo, M. Takahata, S. Tanaka, E. Tcherniaev, E. S. Tehrani, M. Tropeano, P. Truscott, H. Uno, L. Urban, P. Urban, M. Verderi, A. Walkden, W. Wander, H. Weber, J. P. W. T. Wenaus, D. C. Williams, D. Wright, T. Yamada, H. Yoshida, and D. Zschiesche (GEANT4 Collaboration), *Nucl. Instrum. Methods Phys. Res. A* **506**, 250 (2003).
- [12] T. W. Burrows, *Nucl. Data Sheets* **107**, 1747 (2006).
- [13] Z. Elekes, J. Timar, and B. Singh, *Nucl. Data Sheets* **112**, 1 (2011).
- [14] J. Raynal, "Notes on ecis95," CEA Saclay report (1995).
- [15] A. J. Koning and J.-P. Delaroche, *Nucl. Phys. A* **713**, 231 (2003).
- [16] A. M. Bernstein, V. R. Brown, and V. A. Madsen, *Comments Nucl. Part. Phys.* **11**, 203 (1983).
- [17] A. M. Bernstein, V. R. Brown, and V. A. Madsen, *Phys. Lett. B* **103**, 255 (1981).
- [18] B. A. Brown and B. H. Wildenthal, *Phys. Rev. C* **21**, 2107 (1980).
- [19] A. Bohr and B. R. Mottelson, *Nuclear Structure*, Vol. 2 (Benjamin, New York, 1975).